Brief Review

Modern Physics Letters B, Vol. 18, Nos. 26 & 27 (2004) 1327–1345

World Scientific
www.worldscientific.com

THEORETICAL STUDY OF NEUTRAL DIPOLAR ATOM IN WATER: STRUCTURE, SPECTROSCOPY AND FORMATION OF AN EXCITONIC STATE

RICCARDO SPEZIA*, FRANÇOIS-XAVIER COUDERT and ANNE BOUTIN

Laboratoire de Chimie Physique, UMR 8000, CNRS,
Université Paris-Sud XI, 91405 Orsay Cedex, France
**spezia@ens.fr*

Received 29 October 2004

We review theoretical studies on the properties of solvated neutral dipolar atoms. The combination use of mixed quantum classical molecular simulations and analytical mean-field dipolar excitonic state theory allows the rationalization of the experimental observations in terms of physical macroscopic properties. A very good agreement is observed between experiments, theory and simulations on the spectroscopic behavior of silver in water. Molecular simulations also give thermodynamic and kinetic information on the reduction reaction of the cation that leads to the neutral atom in an excitonic state.

Keywords: Excitonic state; hydrated neutral atom; solvated electron; molecular dynamics.

1. Introduction

Cation reduction in solution is an everyday process having a fundamental role in a broad range of fields, from industrial to biological sciences. For this reason, several efforts were done to understand the elementary processes involved. In particular the electron transfer, the crucial step regulating thermodynamically and kinetically redox reactions, was largely investigated during the last decades.[1] Pulse radiolysis of a metal ion in solution offers a powerful method to reduce solvated metal ions by solvated electron and to study by time-resolved spectroscopy the formation of metal atoms and their coalescence.[2]

Different ways can be adopted to generate a solvated electron.[3] Hart and Boag pointed out in water for the first time in 1962[4] the so-called *hydrated* electron, confirming previous hypothesis of its existence.[5] Its absorption spectrum is a non-structured band with a maximum at 1.72 eV. The hydrated electron was largely characterized experimentally, including studies of its stationary spectrum in different conditions.[6] More recently, its formation dynamics became the subject of several

*Present address: Département de Chimie, Ecole Normale Supérieure, UMR 8640, CNRS, 24 rue Lhomond, F-75231 Paris Cedex 05, France.

studies.[7] Furthermore, in last ten years it was the subject of several theoretical and computational studies.[8,9]

Since the solvated electron is a very strong reducing agent, when produced in a solution it is able to reduce cations. Of course, the reduction process is determined by the chemical nature of the cation. Considering, for simplicity, only monovalent cations (similar considerations can be made for other types of cations), when a solvated electron is produced in a solution containing a soluble salt of this cation, two different processes can occur:

$$M^+ + e^-_{\text{sol}} \rightleftharpoons M^0 \tag{1}$$

and

$$M^+ + e^-_{\text{sol}} \rightleftharpoons (M^+, e^-_{\text{sol}})\,. \tag{2}$$

When Reaction (1) is favored, the atoms can dimerize or associate with excess ions

$$M^0 + M^+ \rightleftharpoons M_2^+ \tag{3}$$

and, by a multistep process, these species progressively coalesce into clusters. The most studied reduction reaction assisted by a solvated electron is probably that of the silver cation. It was in fact the first ion aqueous solution studied by pulse radiolysis[10] and was recently revisited.[11,12]

The product of Reaction (1) is a neutral atom in a polar solvent, water generally. Such a state, before reacting with other cations, can be stabilized by an atomic induced dipole moment due to the hybridization of atomic orbitals, achieving a large dipole moment. This large dipole moment can then polarize its neighbors. The resulting reaction field enhances the polarizability of the atom. If there is a sufficient number of neighbors, the reaction field can overcome the energy cost of hybridizing the atom entirely and an effective dipolar atom would result. This stabilized state is called "excitonic state". The transition to an excitonic phase consisting of dipolar atoms was invoked to understand the metal–nonmetal transition in expanded liquid mercury.[13] Fluid lithium can also undergo a similar transition.[14] Another possibility of having a transition to an excitonic state can occur in a variety of impurity-doped matrix systems, like for example low temperature alkali-doped rare gas solids at low impurity concentrations. Such a possibility was described by Logan,[15] considering an alkali atom that, when isolated, contains a single *ns* electron outside a closed shell. He assumed a sufficiently low impurity concentration, so that the impurity-impurity interactions may be neglected. Such conditions are experimentally possible for these systems.[16] Moreover, alkali impurity atoms can be stabilized at low temperatures in solid ammonia or in glasses.[17] Liquid host matrices are also possible: Li atom in liquid ammonia presenting the characteristics of an excitonic state has been observed from path integral quantum Monte Carlo calculations of Sprik *et al.*[18,19] A similar situation was found by quantum/classical and Car–Parrinello molecular dynamics in the case of the neutral silver atom generated in aqueous solution as in Reaction (1).[20]

In this review we show our recent progresses addressed to study Reaction (1) by means of atomistic simulations and mean-field excitonic state theory, examining in particular the case of the silver atom in water. The case of Reaction (2) does not lead to the formation of an excitonic state. It can be computationally studied with the same quantum/classical approach, as was done in the case of sodium,[21] but it cannot be interpreted by means of the same mean-field theory. We will show here only the case of silver, Reaction (1). At this end we employ a mixed quantum/classical molecular dynamics approach based on an adiabatic simulation technique[9] where the solvated electron is treated quantum-mechanically and the cation and bulk water classically, as described in the next section. Within this approach one can obtain the absorption spectrum of the system, that can be directly compared with experiments and excitonic state theory. Finally, some insights into the formation process are shown. They can be obtained putting together information coming from quantum umbrella sampling of the electron–cation association with free simulation aimed to see the spontaneous reactive process.[21,22]

This brief review is organized as follows. In Sec. 2 we give an overview of the computational techniques adopted to have microscopical information about the processes. Then in Sec. 3 we give a short description of the mean-field formulation of the excitonic state transition and we apply it to the case of silver atom in water, comparing theoretical results with information taken from the atomistic simulation and experiments. Finally, in Sec. 4, the reactive process is investigated. The paper ends with general conclusions of our studies at the present stage and perspectives for future investigations.

2. Computational Approaches

The systems under investigation are composed by one monovalent cation, an excess electron and solvent water molecules. When the cation is reduced by the electron, a neutral atom is formed, otherwise a contact pair or, in a limit case, two non-interacting particles are obtained. The formation and the stability of the neutral atom in water can be studied by MD simulations. Different techniques can be employed, generally following the Born–Oppenheimer approximation. A well established way is to use Car–Parrinello molecular dynamics (CPMD),[23] where all the interactions are obtained from first principles. Of course, there will be limitations on both the dimension of the system and the time length of the simulations. Another way is to divide the system in two parts, one described by classical interactions and the other following the Schrödinger equation. Using this quantum/classical molecular dynamics (QCMD) it is possible to avoid some CPMD limitations, although a parametrization of the potential describing the interactions is needed. In this section we present the basics of QCMD that can be used to study the reduction of a cation by an electron in solution. We first describe the interactions between the particles of the system — electron, cation and solvent — then we show the basics of the dynamics and finally the quantum umbrella sampling that can be used to study the reaction leading to the cation reduction by the solvated electron.

2.1. *Definition of the interactions*

Before directly addressing the dynamics, a reasonable description of the interactions between the particles is needed. At this end we adopt an additive perspective for the interactions, where the total potential of the system is given by:

$$V = V_{\mathrm{el/cat}} + V_{\mathrm{el/solv}} + V_{\mathrm{cat/solv}} + V_{\mathrm{solv/solv}} \,, \tag{4}$$

where $V_{\mathrm{el/cat}}$ and $V_{\mathrm{el/solv}}$ represent the electron/cation and electron/solvent interactions respectively. $V_{\mathrm{cat/solv}}$ is the cation/solvent interaction potential and $V_{\mathrm{solv/solv}}$ is the solvent/solvent interaction potential. The two latter terms are considered as pure classical two-body interactions, composed, as in usual classical force fields,[24] by a Coulombic and a Lennard–Jones (LJ) term

$$V_{ij} = \frac{1}{4\pi\epsilon_0}\frac{q_i q_j}{r_{ij}} + 4\epsilon_{ij}\left[\left(\frac{\sigma_{ij}}{r_{ij}}\right)^{12} - \left(\frac{\sigma_{ij}}{r_{ij}}\right)^{6}\right] , \tag{5}$$

where i and j are two interacting atoms holding to different molecules. For the solvent water molecules we adopt the SPC model,[25] while for Ag^+/water interactions there were no LJ parameters in the literature, and hence we adjusted them[20,21] in order to better reproduce structural and energetic properties of silver cations in water.[26]

The electron/solvent and electron/cation interaction energies are evaluated adding in the time-independent Schrödinger equation of the electron two pseudopotential terms, leading to

$$[\hat{T}_e + \hat{V}_{\mathrm{int}}(\mathbf{r}, \mathbf{S})]\psi_n(\mathbf{r}, \mathbf{S}) = E_n(\mathbf{S})\psi_n(\mathbf{r}, \mathbf{S}) \tag{6}$$

where $\hat{T}_e$ denotes the electronic kinetic energy operator, $\mathbf{r}$ the electronic coordinates, $\mathbf{S}$ the solvent-cation configurations, ψ_n the electronic wavefunction and $\hat{V}_{\mathrm{int}}$ the effective electron/solvent-cation interaction potential. The latter is composed by two contributions, the electron/water, $\hat{V}_{\mathrm{el/wat}}$, and the electron/cation, $\hat{V}_{\mathrm{el/cat}}$, pseudopotentials. For $\hat{V}_{\mathrm{el/wat}}$ we use the pseudopotential developed by Turi and Borgis,[27] that is based on a quantum *ab initio* calculation of one water molecule plus an additional electron confined in a box in the static exchange theory limit. It has the following form:

$$\hat{V}_{\mathrm{el/wat}} = \hat{V}_{\mathrm{SE}}(\mathbf{r}, \mathbf{r}_{\mathrm{O}}, \mathbf{r}_{\mathrm{H1}}, \mathbf{r}_{\mathrm{H2}}) + \hat{V}_{\mathrm{pol}}(\mathbf{r}, \mathbf{r}_{\mathrm{O}}) \tag{7}$$

where $\mathbf{r}_{\mathrm{O}}, \mathbf{r}_{\mathrm{H1}}, \mathbf{r}_{\mathrm{H2}}$ are the coordinates of oxygen and hydrogen atoms of water molecules. The first term, $\hat{V}_{\mathrm{SE}}$, takes into account the interactions of the excess electron with the *frozen* molecular orbitals of a given water, having the form:

$$\hat{V}_{\mathrm{SE}} = \hat{V}_{\mathrm{O}}(\mathbf{r}, \mathbf{r}_{\mathrm{O}}) + \hat{V}_{\mathrm{H1}}(\mathbf{r}, \mathbf{r}_{\mathrm{H1}}) + \hat{V}_{\mathrm{H2}}(\mathbf{r}, \mathbf{r}_{\mathrm{H2}}) \tag{8}$$

$$\hat{V}_X = Q_X \frac{\mathrm{erf}(A_X|\mathbf{r} - \mathbf{r}_X|)}{|\mathbf{r} - \mathbf{r}_X|} + B_X \frac{\mathrm{erf}(C_X|\mathbf{r} - \mathbf{r}_X|) - \mathrm{erf}(D_X|\mathbf{r} - \mathbf{r}_X|)}{|\mathbf{r} - \mathbf{r}_X|} \,, \tag{9}$$

where the index X represents either O or H, Q_X is the partial charge of the molecular sites and A_X, B_X, C_X and D_X are adjustable parameters. The second term,

$\hat{V}_{\rm pol}$, is a polarization contribution, accounting for electronic correlation effects, for which we use the form proposed by Barnett *et al.*[28]

$$\hat{V}_{\rm pol} = \frac{\alpha_{\rm W}}{2(|\mathbf{r} - \mathbf{r}_{\rm O}|^2 + r_{\rm p}^2)^2}\,, \tag{10}$$

where $\alpha_{\rm W}$ is the water molecular polarizability and $r_{\rm p}$ a typical atomic length. For the electron/cation pseudopotential we employed the form proposed by Durand and Barthelat[29] with a set of refined parameters for silver.[21] It has the form:

$$\hat{V}_{\rm el/cat} = -\frac{1}{r} + \hat{W}^{\rm ps} \tag{11}$$

where $-(1/r)$ is the Coulombic interaction term and $W^{\rm ps}$ is the nonlocal term of the pseudopotential, given by

$$\hat{W}^{\rm ps} = \sum_l W_l(r)\hat{P}_l\,, \tag{12}$$

$$W_l = e^{-\alpha_l r^2} \sum_{i=1}^{n_l} c_{i,l} r^{n_{i,l}}\,, \tag{13}$$

where $\hat{P}_l$ is the projector on the spherical harmonics Y_{lm}. More details on the pseudopotentials can be found in Refs. 9 and 21.

2.2. *Quantum/classical molecular dynamics*

Using the interaction potentials described in the previous subsection, it is possible to study the electron/cation/water systems using mixed quantum classical molecular dynamics (QCMD). We consider each system as composed by two subsystems, a classical subsystem, the cation and the solvent (water), following classical Newton's equation of motion, and a quantum subsystem, the excess electron, following the Schrödinger equation. Note that the electron is not, strictly speaking, treated quantum-dynamically, since we obtain the electron wavefunction solving the time-independent Schrödinger equation (6). For each classical configuration of the solvent-cation subsystem, we calculate the new electron wavefunction that contributes to the forces acting on the classical subsystem via the Hellman–Feynman theorem,[30] such that:

$$\mathbf{F}_S^{\rm q} = -\nabla_{\mathbf{S}} E_0(\mathbf{S}) = -\int_{-\infty}^{+\infty} d\mathbf{r}\, \psi_0(\mathbf{r},\mathbf{S})^2 \nabla_{\mathbf{S}} \hat{V}_{\rm int}(\mathbf{r},\mathbf{S})\,. \tag{14}$$

In this work we always computed these forces for the ground state of the excess electron ($n = 0$), although an extended usage to excited states is also possible. The single electron wavefunctions $\psi_n(\mathbf{r},\mathbf{S})$ are expanded into a basis of $7 \times 7 \times 7$ spherical Gaussian functions centered on the nodes of a cubic box.

For the classical subsystem we immersed the cation in 300 or 800 SPC water molecules, with the excess electron treated with the Born–Oppenheimer dynamics

described above. Standard periodic boundary conditions are employed to simulate bulk behavior with the Ewald summation technique to calculate electrostatic interactions.[31] The simulations are performed in the NVT ensemble using the Nosé–Hoover thermostat to ensure isothermal conditions.[32] The integration of translation and rotation equations of motion is performed using the Gear predictor-corrector algorithm.[33] The simulation runs have a typical time length of a few tens of picoseconds after a stabilization time.

2.3. *Reaction free energy profile*

Some insights on the cation reduction reaction path can be obtained from QCMD simulations by calculating free energy curves as a function of the electron cation distance, $r_n(\mathbf{S})$, defined as

$$r_n(\mathbf{S}) = |\langle \Psi_n | \mathbf{r} | \Psi_n \rangle - \mathbf{R}_{\text{cat}}| = \xi \,. \tag{15}$$

The distance ξ is the easiest microscopic property given by simulations we can relate to the formation of an excitonic state, coupled with a wavefunction analysis. The limiting situation $\xi = 0$ corresponds to the electron located on the atom. Increasing ξ, we have first a distortion of the atom leading to a dipolar atom (the excitonic state, largely described in the next section), then an electron/cation contact pair is formed, while for larger values of ξ we have two distinct solvated species, the hydrated electron and the cation (see Fig. 1).

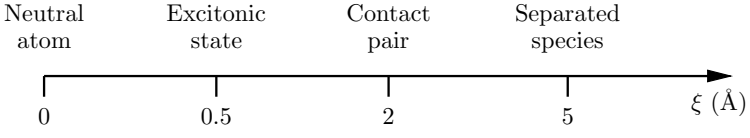

Fig. 1. Schematic representation of different states as a function of the electron cation distance.

Along this coordinate, the free energy function will be given by

$$F_n(\xi) = -k_{\text{B}} T \ln P_n(\xi) \,, \tag{16}$$

where $P_n(\xi)$ is the probability to find the electron in its electronic state n for the electron/cation distance ξ,

$$P_n(\xi) = \langle \delta[r_n(\mathbf{S}) - \xi] \rangle_n \,. \tag{17}$$

The solvent average $\langle \cdots \rangle_n$ and the data points $r_n(\mathbf{S})$ for the reaction coordinate are calculated by QCMD with the total Hamiltonian

$$H_n(\mathbf{S}) = E_n(\mathbf{S}) + \mathcal{H}(\mathbf{S}) \,, \tag{18}$$

where $\mathcal{H}(\mathbf{S})$ is the classical kinetic and potential energy due to the solvent and the cation. To sample the electron cation distances we use the Umbrella Sampling (US) approach, adding the following quadratic potential to the Hamiltonian of Eq. (18):

$$U_{\xi_0} = \frac{1}{2}k[r_n(\mathbf{S}) - \xi_0]^2 \,. \tag{19}$$

The US technique was adapted for the case of a system including a quantum particle by Borgis and Staib[34] and this methodology was succesfully used in the case of the cations reduction process.[21,22]

3. Dipolar Excitonic State

In this section we briefly review the basic concepts of the mean-field dipolar excitonic state theory based on works of Logan and coworkers[15,35] with a particular focus on the application to a neutral atom in a liquid host matrix and the specific case of silver in water. From excitonic state theory it is possible to obtain the hybridized atomic orbitals and hence the atomic wavefunctions of the states considered. The induced silver dipole and electronic transitions between s and p states can thus be evaluated and directly compared with QCMD results and experimental data.

3.1. *General theory*

Considering an atom containing a single ns electron outside a closed shell, like elements of groups 1 (alkali atoms) and 11 (for instance, silver), it is possible to write the isolated atom Hamiltonian considering simply a single ns orbital with energy $\epsilon_0 = -\hbar\omega_0$ and three np orbitals, with energy $\epsilon_1 = \hbar\omega_0$. Neglecting higher excited states, the atomic Hamiltonian is therefore reduced to a simple four-level system (FLS) that can be represented by

$$\hat{H}_0 = \hbar\omega_0 \left(-|s\rangle\langle s| + \sum_\alpha |p_\alpha\rangle\langle p_\alpha| \right), \tag{20}$$

where $\alpha = x, y$ or z. An external electric field will introduce the perturbation $\hat{H}_E = -\hat{\boldsymbol{\mu}} \cdot \mathbf{E^0}$, where $\hat{\boldsymbol{\mu}}$ is the dipole moment operator. In the above basis the perturbation Hamiltonian is given by

$$\hat{H}_E = \hbar \sum_\alpha (|s\rangle\langle p_\alpha| + |p_\alpha\rangle\langle s|)\xi_\alpha \,, \tag{21}$$

where $\hbar\xi_\alpha = ME^0_\alpha$ represents the energy contribution due to the external field and $M = \langle s|\hat{\mu}_\alpha|p_\alpha\rangle$ is the transition dipole moment. The new Hamiltonian, $\hat{H}_0 + \hat{H}_E$, can be diagonalized leading to four eigenvalues, $\hbar\omega^0_-$, $\hbar\omega_0$ (doubly degenerate) and $\hbar\omega^0_+$, where

$$\omega^0_\pm = \pm\sqrt{\omega_0^2 + \xi^2} \tag{22}$$

and the corresponding normalized, orthogonal eigenfunctions are given by

$$|\Psi_-^0\rangle = |s + \lambda p_0\rangle[1 + \lambda^2]^{-1/2} \tag{23}$$

$$|\psi_0^0\rangle = |p_1\rangle \text{ and } |p_{-1}\rangle \tag{24}$$

$$|\psi_+^0\rangle = |p_0 - \lambda s\rangle[1 + \lambda^2]^{-1/2} \tag{25}$$

where

$$\lambda = \frac{(\omega_0^2 + \xi^2)^{1/2} - \omega_0}{|\xi|}\,. \tag{26}$$

Since the new (perturbed) wavefunctions are obtained, one can express the new (perturbed) transition dipole moments in this basis, giving

$$\langle\Psi_-^0|\hat{\boldsymbol{\mu}}|\psi_+^0\rangle = \frac{1 - \lambda^2}{1 + \lambda^2}\mathbf{M} \tag{27}$$

$$\langle\Psi_-^0|\hat{\boldsymbol{\mu}}|\psi_0^0\rangle = \frac{1}{(1 + \lambda^2)^{1/2}}\mathbf{M}\,. \tag{28}$$

We can now consider that the atom (the impurity) is immersed in an inert (nonreactive) condensed phase matrix, solid or liquid. Assuming a sufficiently low concentration of the impurity, we can neglect impurity–impurity interactions, thus considering a single matrix-bound impurity. The mean-field theory we are going to shortly review here is based on the following assumptions:

(i) the impurity atom valence electron remains strongly localized;
(ii) the $ns \rightarrow np$ excitations in the matrix-bound impurity are of Frenkel type;
(iii) there is no overlap with the host matrix absorption bands.

Following the continuum dielectric theory,[36] we can express the local field acting on the matrix-bound impurity, $\mathbf{f}(\mathbf{E})$, as given by two contributions:

$$\mathbf{f}(\mathbf{E}) = \mathbf{G}(\mathbf{E}) + \mathbf{R}(\mathbf{E}; \langle\boldsymbol{\mu}\rangle) \tag{29}$$

where $\mathbf{G}(\mathbf{E})$ is the electric field inside the cavity due to external sources and $\mathbf{R}(\mathbf{E}; \langle\boldsymbol{\mu}\rangle)$ is the reaction field due to the total impurity dipole moment, $\boldsymbol{\mu}$, that polarizes its surrounding. Hence, the mean-field interaction Hamiltonian, $\hat{H}_{\text{int}}$, can be expressed as

$$\hat{H}_{\text{int}} = -\hat{\boldsymbol{\mu}} \cdot \mathbf{f}(\mathbf{E}) \tag{30}$$

$$= -\hat{\boldsymbol{\mu}} \cdot \left[\frac{3\epsilon_m}{2\epsilon_m + 1}\mathbf{E} + g(\rho_m)\langle\boldsymbol{\mu}\rangle\right]\,, \tag{31}$$

where $g(\rho_m)$ is the reaction field factor

$$g(\rho_m) = \frac{8\pi\rho_m}{3}\frac{(\epsilon_m - 1)}{(\epsilon_m + 1)} \tag{32}$$

with ρ_m and ϵ_m being the matrix density and dielectric constant respectively. Hence, the effective Hamiltonian, $\hat{H}_i$, will be given by

$$\hat{H}_i = \hat{H}_0 + \hat{H}_{\text{int}} \,. \tag{33}$$

To obtain $\hat{H}_{\text{int}}$ from Eq. (31) we should know $\langle \boldsymbol{\mu} \rangle$, the impurity dipole moment, that, as the expectation value of any quantum operator, is given by

$$\langle \boldsymbol{\mu} \rangle = Q_i^{-1} \, \text{Tr} \{ \hat{\boldsymbol{\mu}} \exp[-\beta \hat{H}_i(\langle \boldsymbol{\mu} \rangle)] \} \,, \tag{34}$$

where Tr is over the eigenstates of $\hat{H}_i = \hat{H}_0 + \hat{H}_{\text{int}}$.

We have hence a self-consistent equation for the matrix-bound impurity dipole moment. The solution for $\langle \boldsymbol{\mu} \rangle$ will be a function of both the atomic properties of the free impurity and the thermodynamic properties of the host matrix, i.e. the environment. In the absence of an applied external electric field ($\mathbf{E} = 0$), the self-consistent equation for $\langle \boldsymbol{\mu} \rangle$ is

$$\langle \boldsymbol{\mu} \rangle_0 y(\langle \mu \rangle_0) = \langle \boldsymbol{\mu} \rangle_0 \frac{\tanh[\beta s(\rho_m) y(\langle \mu \rangle_0)]}{1 + \exp(-\beta \hbar \omega_0) \, \text{sech}[\beta s(\rho_m) y(\langle \mu \rangle_0)]} \tag{35}$$

with

$$y(\langle \mu \rangle_0) = [\alpha_0 g(\rho_m)]^{-1} \sqrt{1 + \frac{\alpha_0}{\hbar \omega_0} [g(\rho_m) \langle \mu \rangle_0]^2} \,, \tag{36}$$

where α_0 is the polarizability of the FLS and

$$s(\rho_m) = \hbar \omega_0 \alpha_0 g(\rho_m) > 0 \,. \tag{37}$$

Note that to solve Eq. (35) one has only to know the properties that characterize the isolated impurity atom, α_0 and ω_0, and the host matrix, ρ_m and ϵ_m. One solution of Eq. (35) is the trivial one, $\langle \boldsymbol{\mu} \rangle_0 = 0$, corresponding to the absence of an atomic dipole. Moreover, given the atomic properties α_0 and ω_0, at a fixed temperature, a critical density $\rho_{m,c}$ exists such that for $\rho_m < \rho_{m,c}$ only the trivial solution $\langle \boldsymbol{\mu} \rangle_0 = 0$ can fulfil the self-consistent equation (35). On the other hand, for $\rho_m > \rho_{m,c}$, two solutions are possible: $\langle \boldsymbol{\mu} \rangle_0 = 0$ and $\langle \boldsymbol{\mu} \rangle_0 > 0$, where the latter is favored thermodynamically. Hence, for $\rho_m = \rho_{m,c}$ the system has a transition to a dipolar excitonic state, $\langle \boldsymbol{\mu} \rangle_0 > 0$.

A simplified expression of the self-consistent equation (35) can be obtained for the limit situation $y(\langle \mu \rangle_0) \to 1$, leading to

$$\frac{\langle \mu \rangle_0^2}{M^2} = \frac{[\alpha_0 g(\rho_m)]^2 - 1}{[\alpha_0 g(\rho_m)]^2} \tag{38}$$

that preserves all the features of a transition to a dipolar excitonic state, and that was conveniently used to analyze the presence of a dipolar excitonic state in liquid systems.[19,20]

3.2. *Dipolar atom properties*

Once the excitonic state is obtained, the original atomic properties will of course be changed. These changes can be thought in terms of hybridization of original s and p orbitals, leading to the wavefunction

$$|\Psi(\tilde{\lambda})\rangle = |S + \tilde{\lambda} P_z\rangle (1 + \tilde{\lambda}^2)^{-1/2} , \tag{39}$$

and the sp-hybrid state will have the following dipole moment

$$\langle \mu_\alpha \rangle_0 = \langle \Psi(\tilde{\lambda}) | \hat{\mu}_\alpha | \Psi(\tilde{\lambda}) \rangle \tag{40}$$

$$= \frac{2\tilde{\lambda} M}{(1 + \tilde{\lambda}^2)} \delta_{\alpha z} , \tag{41}$$

where $\tilde{\lambda}$ is a mixing coefficient that can be regarded here as a parameter. It will be useful to express the total free energy change of the system associated to the formation of the dipolar atomic state as a function of $\tilde{\lambda}$, taking as reference the normal state, $\langle \boldsymbol{\mu} \rangle_0 = 0$, where $\tilde{\lambda} = 0$. This total free energy change, $\Delta A(\tilde{\lambda})$, is composed by two contributions: (i) the hybridization free energy cost, $A_h(\tilde{\lambda})$, and (ii) the free energy arising from the interaction with the environment, $A_s(\tilde{\lambda})$. Then the total free energy change, $\Delta A(\tilde{\lambda}) = A_h(\tilde{\lambda}) + A_s(\tilde{\lambda})$, will be given by

$$\Delta A(\tilde{\lambda}) = 2\hbar\omega_0 \frac{\tilde{\lambda}^2}{(1 + \tilde{\lambda}^2)} \left[1 - \frac{\alpha_0 g(\rho_m)}{(1 + \tilde{\lambda}^2)} \right] . \tag{42}$$

Note that for $\rho_m < \rho_{m,c}$, $\Delta A(\tilde{\lambda})$ has a minimum at $\tilde{\lambda} = 0$, i.e. the normal state is the stable state; on the other hand for $\rho_m \geq \rho_{m,c}$, $\Delta A(\tilde{\lambda})$ has a minimum for

$$\lambda^2 = \frac{\alpha_0 g(\rho_m) - 1}{\alpha_0 g(\rho_m) + 1} . \tag{43}$$

Once the dipolar excitonic state is formed ($\rho_m > \rho_{m,c}$) the energies of the perturbed states described by $|\Psi_-\rangle$ and $|\psi_+^0\rangle$ in Eqs. (23) and (25) will be split by

$$\Delta_{EI} = \omega_0 \left(\left\{ 1 + \frac{\alpha_0}{\hbar\omega_0} \left[g(\rho_m) \langle \mu \rangle_0 \right]^2 \right\}^{1/2} - 1 \right) \tag{44}$$

such that

$$\omega_\pm = \pm(\omega_0 + \Delta_{EI}) . \tag{45}$$

One can interpret microscopic observations taken from simulations in terms of a mean-field theory based on experimental observables (i.e. an essentially macroscopic theory). In particular the average dipole moment of the impurity can be obtained from MD simulations. This kind of study was done originally by Logan[19] where he analyzed a simulation study (Sprik *et al.*,[18]) of Li in ammonia in which he pointed out that the simple Eq. (38) can predict the formation of an atomic dipole of Li, obtaining a good quantitative agreement with results found in the atomistic simulation. More recently, the behavior of neutral silver atom in water was studied

by two independent and different atomistic simulations, CPMD and QCMD.[20] Also in this case a neutral dipolar atom is formed, i.e. an excitonic state, providing a good agreement between theory and simulations (notably 1.96 D from theory versus 1.9 D and 2.4 D obtained from CPMD and QCMD respectively). This state is also particularly interesting from the point of view of the solvent structures. In fact it mainly presents the typical features of a solvated neutral species, but the solvent is partly organized to stabilize the atomic induced dipole, that adiabatically follows the electric field applied by the solvent.[20] As has been already pointed, the silver cation is reduced by the electron in water solution leading to a dipolar atom, that can be well interpreted as an excitonic state. From the same kind of atomistic simulations we also noticed that replacing silver cation with sodium cation a different situation is obtained.[21] Changing the chemical nature of the cation, sodium now, it is no more reduced, as expected, and only a metastable cation/electron contact pair is formed with an average distance of ~ 2 Å. This metastable contact pair was also found by Laria and Kapral in micelles[37] and its presence was suspected by experiments[38] — of course being a metastable state, it is experimentally difficult to detect. In this case the basic assumptions of the excitonic theory are no more valid, for example simply because the *s* electron is no more localized on the atom.

3.3. *Electronic transitions*

Systems where an excess electron is formed in solution in presence of cations are generally investigated experimentally via electronic spectroscopy.[12,39] It is evident, from Eqs. (23)–(25) and (44)–(45), that excitonic theory is in principle able to provide transition energies between ns and np states of the impurity. To fully investigate the spectroscopic consequences of a transition to an excitonic state, at least two effects must be incorporated in the theory: the spin–orbit coupling interaction and the spatially local, primarily repulsive interactions (corresponding to the usual van der Waals classical repulsive short range interactions). Hence, the Hamiltonian $\hat{H}_i$ of Eq. (33) is replaced by

$$\hat{H}'_{\text{int}} = \hat{H}_i + \hat{H}_{\text{so}} + \hat{V}_0 \tag{46}$$

where $\hat{H}_{\text{so}}$ is the spin–orbit coupling Hamiltonian and $\hat{V}_0$ is a spherically symmetric interaction term taking into account the local interactions that do not mix the ns and np orbitals.

Then, it is possible to write simple expressions for the total resulting transition energies

$$\Delta E_1 = E_0 + \delta + \frac{3}{2}\Delta_{EI} - \frac{1}{4}\zeta - \frac{1}{2}\left(\Delta_{EI}^2 + \zeta\Delta_{EI} + \frac{9}{4}\zeta^2\right)^{1/2}, \tag{47}$$

$$\Delta E_2 = E_0 + \delta + \Delta_{EI} + \frac{1}{2}\zeta, \tag{48}$$

$$\Delta E_3 = E_0 + \delta + \frac{3}{2}\Delta_{EI} - \frac{1}{4}\,\zeta + \frac{1}{2}\left(\Delta_{EI}^2 + \zeta\Delta_{EI} + \frac{9}{4}\,\zeta^2\right)^{1/2}, \qquad (49)$$

where $E_0 = 2\hbar\omega_0$, ζ is an effective np spin–orbit coupling constant and δ is the energy shift between ns and np orbitals due to $\hat{V}_0$ (i.e. $\delta = \langle p|\hat{V}_0|p\rangle - \langle s|\hat{V}_0|s\rangle$). Note that Eqs. (47)–(49) contain the normal state ($\Delta_{EI} = 0$, $\Delta E_2 = \Delta E_3$) and the excitonic state ($\Delta_{EI} \neq 0$).

To directly address the transition energies from Eqs. (47)–(49), δ is probably the most problematic term to estimate. It is also a crucial value, since, disregarding it, the theory can provide only blue-shifted spectra. If a red-shifted spectrum is observed, it can be justified by a negative δ that balances a positive Δ_{EI}. Unfortunately, δ cannot be obtained analytically but only via semi-empirical considerations. In the case of silver we can make a first drastic, but reasonable assumption considering $\delta_p \ll \delta_s$ and then $\delta = -\delta_s$. This term, δ_s, can be further estimated from the energy of $|S\rangle$ state *in vacuo*, $E_{\text{vac}}^{|S\rangle}$, and in solution, $E_{\text{sol}}^{|S\rangle}$, as obtained from simulations reported in Ref. 21, and using Δ_{EI} via Eq. (44) as the electrostatic contribution of the solvent. Thus,

$$\delta_s = E_{\text{sol}}^{|S\rangle} - E_{\text{vac}}^{|S\rangle} + \hbar\Delta_{EI}\,. \qquad (50)$$

The spin–orbit contribution can be taken from recent experimental data.[40] Using the values listed in Table 1 for Ag^0 in water, we can obtain the three transition energies: $\Delta E_1 = 3.33$ eV (372 nm), $\Delta E_2 = 3.51$ eV (353 nm) and $\Delta E_3 = 3.75$ eV (331 nm). All these values are in good agreement with experimental observations.[12] Moreover from QCMD simulations we can obtain as well the overall spectrum of Ag^0 in water that is in good agreement with experiments and also with the previous theoretical considerations (see Fig. 2).

Table 1. Parameters adopted and values obtained to study the excitonic state of silver atom in water at ambient conditions.

Property	Value
α_{Ag}	7.9 Å^3
M_{Ag}	4.8 D
ω_0	15082.9 cm^{-1}[(a)]
ζ	613.8 cm^{-1}[(a)]
ϵ_m	78.3
ρ_m	1.000 g/cm^3
Δ_{EI}	1380.3 cm^{-1}[(b)]
δ_s	3548.9 cm^{-1}[(c)]

[(a)] Experimental value from Ref. 40.
[(b)] Calculated from Eq. (44).
[(c)] Calculated from Eq. (50).

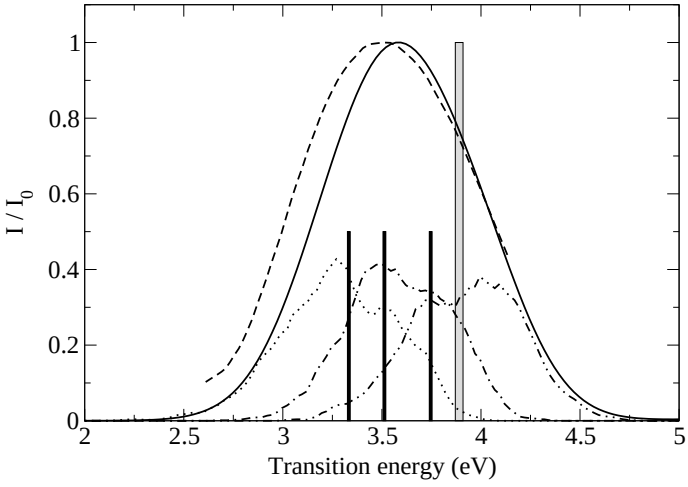

Fig. 2. Absorption spectrum of silver atom in bulk water: experimental (*dashed line*), calculated from QCMD simulations (*solid line*) and obtained from excitonic state theory (*vertical black lines*). The three components obtained from QCMD simulations are separately shown (*dotted*, *dashed-dotted* and *dashed-dotted-dotted*) corresponding to $s \rightarrow p$ transitions. The in-vacuum transition is also shown (*vertical gray bar*).

4. Formation Reactions

In this section we show how it is possible to obtain via atomistic simulations some information on the reactive process between the solvated electron and a cation in water solution. Generally speaking, one can be interested in equilibrium thermodynamics or kinetics properties. In the former case the quantum Umbrella Sampling described in Sec. 2.3 can be used in order to have the free energy profile of the reaction. This is useful mainly to locate the stable state along an electron/cation distance coordinate, as defined in Eq. (15). As expected, this free energy curve presents a clear minimum for electron/silver distance ~ 0.5 Å, as shown in Fig. 3 (for comparison, the free energy curve for a sodium cation is also plotted). This corresponds to the average distance obtained from unconstrained simulations of the excitonic state described previously. It is also possible to show, from a simple thermodynamic cycle, that the free enthalpy of reduction, ΔG^*, is $+0.96$ eV and -0.74 eV for sodium and silver, respectively.[22] These values show that the reduction is thermodynamically favorable for silver and not for sodium. In addition, another important thermodynamic information comes out from umbrella sampling calculations, namely the free energy barrier to escape from the stable state. In the case of silver it was interesting to note that the atomic excitonic state presents a high barrier (over 40 $k_B T$), confirming that this state is both thermodynamically and kinetically stable.

Unfortunately, a full quantitative kinetic information cannot be directly addressed from these curves, since they correspond to an equilibrium solvation

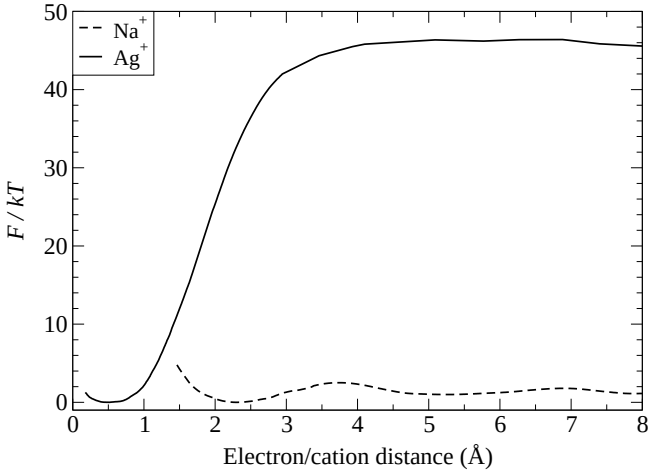

Fig. 3. Free energy profiles as a function of electron cation distance obtained for silver (*solid*) and sodium (*dashed*) cations.

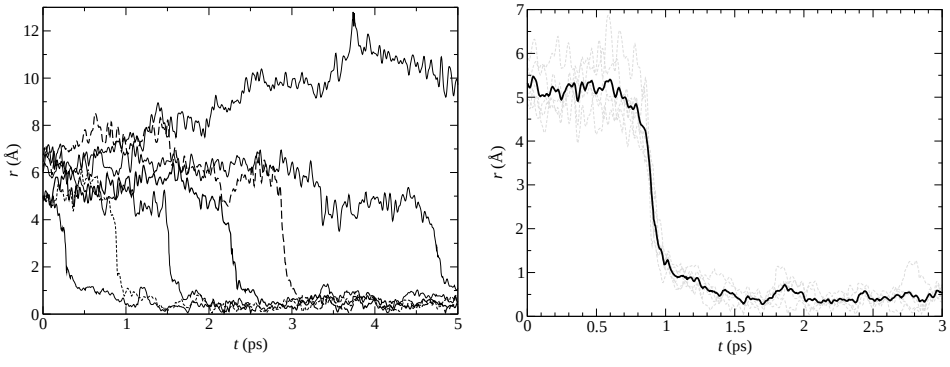

Fig. 4. Electron/cation distance as a function of time during unconstrained simulations of the reduction process. On the right panel, trajectories have been shifted in time; the bold curve is the mean of all trajectories.

regime[41] that assumes the solvent instantaneously relaxing into an equilibrium state. As a consequence, they lack a solvent coordinate that, consistently with Marcus theory for electron transfer,[1] should be employed to fully describe the reaction process.

However, a large barrier in the free energy curve can tell us, qualitatively, that the thermal reaction leading to a separated cation electron state is kinetically unfavored, but a quantitative calculation of kinetic constants needs more effort. Anyway, in the present case we can be sufficiently convinced that this state is kinetically stable other than thermodynamically. Doing independent free QCMD simulations at different starting distances $d_0 \geq 4$ Å, we can obtain some insights into the reduction process (see Fig. 4). In fact, it is possible to decompose the silver reduction process

into the following steps:

(I) a *diffusive* (brownian) step where the electron cation distance reaches a value of ~ 4 Å,
(II) a solvent-solute organization step that allows a rapid jump of the electron to a distance of ~ 1 Å, occurring in ~ 0.15 ps and
(III) a relatively slow decrease of this distance until the formation of the excitonic state, occurring in ~ 0.8 ps.

Note that the timescale of the nondiffusive processes we identified above (i.e. the last two steps) are in agreement with the experimental hypothesis that the reaction should occur in less than 1 ps.[12]

To identify the nature of the system between steps II and III, that we will call the "reduction intermediate state", we have calculated the absorption spectrum (Fig. 5) and the radial density distributions around silver (Fig. 6) by an average over the first 200 fs of step III of all the trajectories. Comparing the spectrum with those of a free hydrated electron and of the silver excitonic state, we see that its maximum is close to the silver excitonic state, while its width is closer to the free hydrated electron. Moreover, the study of radial density distributions reveals that this intermediate state has a weak solvation structure. The first peak of the oxygen radial distribution function is still well-defined but no orientational order is observed. We interpret these results as a rotational reorganization of the solvation structure, with water molecules still presenting a configuration reminiscent of the cation solvation structure. Thus, we can think that the electron rapid jump on the silver cation (step II) is initiated by a favorable configuration of the fluctuating orientation of water molecules around the cation.

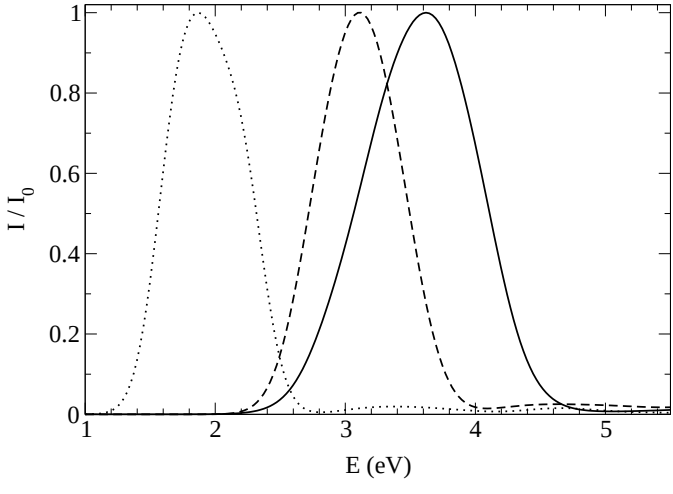

Fig. 5. Absorption spectrum of the excess electron in the reduction intermediate state (*dashed line*), compared to the Ag excitonic state (*solid line*) and the free hydrated electron (*dotted line*).

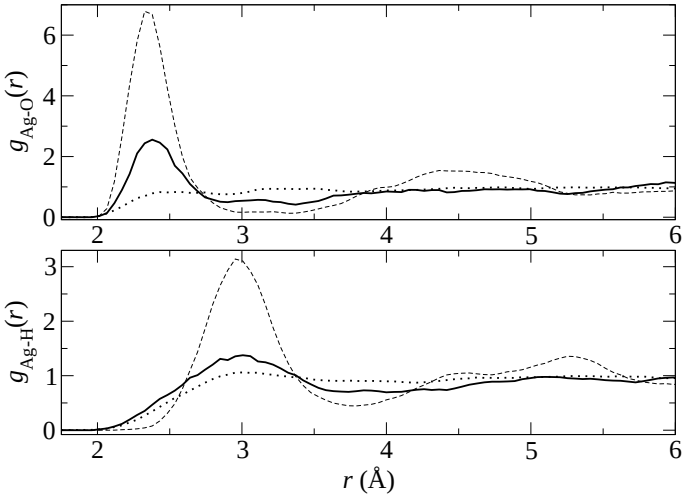

Fig. 6. Radial density functions for oxygen (*upper panel*) and hydrogen (*lower panel*) around the silver atom in the reduction intermediate state (*thick line*), compared to the silver excitonic state (*thin line*) and the Ag^+ cation (*dashed line*).

5. Conclusions and Perspectives

We have reviewed our recent progresses in understanding the formation and stability of neutral atoms in water. In particular, we have shown that it is possible to better understand the physico-chemical basis of such phenomena from both atomistic simulations and theoretical analysis. This combination is particularly interesting to rationalize the microscopic results in terms of physical macroscopic properties. We have studied the simplest reduction process, i.e. the direct interaction between a cation, the reducible species, and the electron, the reducent, in solution. We have found, in the case of silver, that the stationary state we obtained from simulations, the excitonic state, was in good agreement with experimental studies, done in the same thermodynamic conditions, and theoretical analysis. In particular, atomistic simulations are able to well-reproduce experimental UV-Vis spectra of such systems. This is particulary encouraging in order to extend the research to other similar systems, like other cations in solution and in confined systems.

We have shown that the use of mean-field excitonic theory is also useful to shed some light on spectroscopic data. We have obtained a nice agreement between experiments, theory and simulations. This result can give us the basis to investigate with a sufficient degree of confidence the formation of such neutral atoms in different thermodynamic states (of particular interest can be the supercritical conditions). It can be also used to predict the spectroscopic behavior of other atoms in the future.

Finally, we have shown that we can have a general picture of the overall reactive processes, from both constrained — the umbrella sampling studies — and unconstrained simulations. This gives us a first picture of the elementary reduction reaction. To better understand this point, we are going to complete the studies we

have done with other techniques aimed to simulate complex reactions[42] and also, from the theoretical point of view, with a more detailed study of non-equilibrium solvation effects.

Acknowledgments

We wish to acknowledge C. Nicolas, R. Vuilleumier and P. Archirel for fruitful collaborations in this project and D. Borgis, M. Mostafavi, B. Lévy and A. H. Fuchs for several interesting discussions. We thank the Institut du Développement et des Ressources en Informatique Scientifique (IDRIS) of the CNRS for generous allocations of computer time. R. S. would like to thank J. T. Hynes for encouragement and support and CNRS/DFG and European Union through the Marie Curie project for funding.

References

1. R. A. Marcus, *J. Chem. Phys.* **24** (1956) 966; R. A. Marcus and N. Sutin, *Biochim. Biophys. Acta* **811** (1985) 265; M. D. Newton and N. Sutin *Ann. Rev. Phys. Chem.* **35** (1984) 437.
2. J. H. Baxendale and F. Busi, *The Study of Fast Processes and Transient Species by Electron Pulse Radiolysis*, NATO ASI Ser. 86 (D. Reidel Publishing Co., Dordrecht, 1982).
3. E. J. Kirschke and W. L. Jolly, *Inorg. Chem.* **6** (1967) 866; O. H. Leblanc, *J. Chem. Phys.* **30** (1959) 1443; J. Belloni, G. van Amerongen, M. Herlem, J. L. Sculfort and R. Heindl, *J. Phys. Chem.* **84** (1980) 1269; R. Laenen and T. Roth, *J. Mol. Struct.* **598** (2001) 37.
4. E. J. Hart and J. W. Boag, *J. Am. Chem. Soc.* **84** (1962) 4090.
5. J. Jortner, *J. Chem. Phys.* **27** (1957) 823; *ibid.* **30** (1959) 839.
6. E. J. Hart, B. D. Michael and K. H. Schmidt, *J. Phys. Chem.* **75** (1971) 2798; H. Christensen and K. Sehested, *ibid.* **90** (1986) 186; G. Wu, Y. Katsumura, Y. Muroya, X. Li and Y. Terada, *Chem. Phys. Lett.* **325** (2000) 531.
7. A. Migus, Y. Gaudel, J. L. Martin and A. Antonetti, *Phys. Rev. Lett.* **58** (1987) 1559; F. H. Long, H. Lu and K. B. Eisenthal, *ibid.* **64** (1990) 1469; C. Silva, P. K. Walhout, K. Yokoyama and P. F. Barbara, *ibid.* **80** (1998) 1086; M. Assel, R. Laenen and A. Laubereau, *J. Chem. Phys.* **111** (1999) 6869; M. Assel, R. Laenen and A. Laubereau, *J. Phys. Chem.* **A102** (1998) 2256; M. Assel, R. Laenen and A. Laubereau, *Chem. Phys. Lett.* **317** (2000) 13.
8. T. H. Murphey and P. J. Rossky, *J. Chem. Phys.* **99** (1993) 515; B. J. Schwartz and P. J. Rossky, *ibid.* **101** (1994) 6902; *ibid.* **101** (1994) 6917; *Phys. Rev. Lett.* **72** (1994) 3282; A. Staib and D. Borgis, *J. Chem. Phys.* **103** (1995) 2642; D. Borgis and S. Bratos, *J. Mol. Struct.* **436–7** (1997) 537; M. Boero, M. Parrinello, K. Terakura, T. Ikeshoji and C. C. Liew, *Phys. Rev. Lett.* **90** (2003) 226403.
9. C. Nicolas, A. Boutin, B. Lévy and D. Borgis, *J. Chem. Phys.* **118** (2003) 9689.
10. J. H. Baxendale, E. M. Fielden, J. P. Keene and M. Ebert, in *Pulse Radiolysis*, eds. J. P. Keene, A. Swallow and J. H. Baxendale (Academic Press, London, 1965), pp. 207–220; R. Tausch-Treml, A. Henglein and J. Lilie, *Ber. Bunsenges. Phys. Chem.* **82** (1978) 1343; J. Von Pukies, W. Roebke and A. Henglein, *ibid.* **72** (1968) 842; M. Mostafavi, J. L. Marignier, J. Amblard and J. Belloni, *Radiat. Phys. Chem.* **34** (1989) 605.

11. P. Mulvaney and A. Henglein, *Chem. Phys. Lett.* **168** (1990) 391; E. Janata, A. Henglein and B. G. Ershov, *J. Phys. Chem.* **98** (1994) 10888; E. Janata, J. Lilie and M. Martin, *Radiat. Phys. Chem.* **43** (1994) 353.
12. M. Mostafavi, M. Lin, G. Wu, Y. Katsumura and Y. Muroya, *J. Phys. Chem.* **A106** (2002) 3123.
13. W. Hafner and F. Hensel, *Phys. Rev. Lett.* **48** (1982) 1026; L. A. Turkevich and M. H. Cohen, *ibid.* **53** (1984) 2323; L. A. Turkevich and M. H. Cohen, *J. Phys. Chem.* **88** (1984) 3751.
14. D. E. Logan and P. P. Edwards, *Philos. Mag.* **B53** (1986) L23; D. E. Logan and P. P. Edwards, *Ber. Bunsenges. Phys. Chem.* **90** (1986) 575.
15. D. E. Logan, *J. Chem. Phys.* **86** (1987) 234.
16. N. Schwentner, E.-E. Koch and J. Jortner, *Electronic Excitations in Condensed Rare Gases* (Springer, Heidelberg, 1985).
17. P. F. Meier, R. H. Hauge and J. L. Margrave, *J. Am. Chem. Soc.* **100** (1978) 2108; R. Catterali and P. P. Edward, *Chem. Phys. Lett.* **42** (1976) 540.
18. M. Sprik, R. W. Impey and M. L. Klein, *Phys. Rev. Lett.* **56** (1986) 2326.
19. D. R. Logan, *Phys. Rev. Lett.* **57** (1986) 782.
20. R. Spezia, C. Nicolas, A. Boutin and R. Vuilleumier, *Phys. Rev. Lett.* **91** (2003) 208304.
21. R. Spezia, C. Nicolas, P. Archirel and A. Boutin, *J. Chem. Phys.* **120** (2004) 5261.
22. R. Spezia, C. Nicolas, F.-X. Coudert, P. Archirel, R. Vuilleumier and A. Boutin, *Mol. Simul.* **30** (2004) 749.
23. R. Car and M. Parrinello, *Phys. Rev. Lett.* **55** (1985) 2471; J. Hutter, A. Alavi, T. Deutsch, M. Bernasconi, S. Goedecker, D. Marx, M. Tuckerman and M. Parrinello, CPMD version 3.5, MPI Solid State Research Institute in Stuttgart and the IBM Research Laboratory, Zurich (2000).
24. S. J. Weiner, P. A. Kollman, D. A. Case, U. C. Singh, C. Ghio, G. Alagona, S. Profeta and P. Weiner, *J. Am. Chem. Soc.* **106** (1984) 765; W. F. van Guensteren and H. J. C. Berendsen. *Gromos Manual*, BIOMOS, Biomolecular Software, Laboratory of Physical Chemistry, University of Groeningen, The Netherlands (1988).
25. H. J. C. Berendsen, J. P. M. Postma, W. F. van Gunsteren and J. Hermans, in *Interaction Models for Water in Relation to Protein Hydratation* (Reidel, Dordrecht, 1981).
26. N. T. Skipper and G. W. Neilson, *J. Phys.: Condens. Matt.* **1** (1989) 4141.
27. L. Turi and D. Borgis, *J. Chem. Phys.* **117** (2002) 6186.
28. R. N. Barnett, U. Landman and C. L. Cleveland, *J. Chem. Phys.* **88** (1988) 4421; *ibid.* **88** (1988) 4429; R. N. Barnett, U. Landman and A. Nitzan, *ibid.* **90** (1989) 4413.
29. P. Durand and J. C. Barthelat, *Theor. Chim. Acta* **38** (1975) 283.
30. J. Hellmann, *Einführung in die Quantenchemie* (Deuticke, Leipzig, 1937); R. P. Feynman, *Phys. Rev.* **56** (1939) 340.
31. M. P. Allen and D. J. Tildesley, *Computer Simulation of Liquids* (Oxford University Press, Oxford, 1987).
32. S. Nosé, *J. Chem. Phys.* **81** (1984) 511; W. G. Hoover, *Phys. Rev.* **A31** (1985) 1695.
33. C. Gear, *Numerical Initial Value Problems in Ordinary Differential Equations* (Englewood Cliffs, NJ, 1971).
34. D. Borgis and A. Staib, *J. Chem. Phys.* **104** (1996) 4776.
35. M. D. Winn and D. E. Logan, *J. Phys.: Condens. Matt.* **5** (1993) 3103.
36. H. Fröhlich, *Theory of Dielectrics* (Oxford University, Oxford, 1958).
37. D. Laria and R. Kapral, *J. Chem. Phys.* **16** (2002) 7712.
38. H. Gelabert and Y. Gaudel, *J. Phys. Chem.* **100** (1996) 13993.

39. P. Mulvaney and A. Henglein, *Chem. Phys. Lett.* **168** (1990) 391.
40. J. C. Pickering and V. Zilio, *Eur. Phys. J.* **D13** (2001) 181.
41. H. J. Kim and J. T. Hynes, *J. Phys. Chem.* **94** (1990) 2736; *J. Chem. Phys.* **93** (1990) 5194; *ibid.* **93** (1990) 5211; *ibid.* **96** (1990) 5088.
42. M. Iannuzzi, A. Laio and M. Parrinello, *Phys. Rev. Lett.* **90** (2003) 238302.